J. Coat. Technol. Res., **16** (3) 835–845, 2019
https://doi.org/10.1007/s11998-018-00156-4

Synergistic effect of Ag and ZnO nanoparticles on polyaniline incorporated epoxy/2pack coatings for splash zone applications

Mohammad Asif Alam, Ubair Abdus Samad, El-Sayed M. Sherif, Asiful Seikh, Saeed M. Al-Zahrani, Nabeel H. Alharthi, Manawwar Alam

Abstract In this work, epoxy/2pack coatings containing polyaniline (PANI) in combination with Ag and ZnO nanoparticles have been synthesized. The nanoparticles were incorporated with bisphenol-A diglycidyl ether epoxy resin and polyamino-amide. The mechanical properties of the fabricated coatings, such as the pendulum hardness, scratch resistance, and impact strength, were studied. The composition of the fabricated coatings was confirmed by attenuated total reflectance infrared spectroscopy measurements. The thermal degradation and indentations were characterized through the use of differential scanning calorimetry and nano-indentation techniques, respectively. The surface morphology of the fabricated coatings was characterized using field-emission scanning electron microscopy. The synergistic effects of the Ag and ZnO nanoparticles on the corrosion resistance of the coatings after different exposure periods in 3.5% NaCl solutions were determined by electrochemical impedance spectroscopy. All the results were consistent with one another and confirmed that the addition of Ag and ZnO nanoparticles improved the mechanical properties of the coatings. This effect also led to a notable increase in the corrosion resistance of the PANI coatings.

Keywords Epoxy coatings, Polyaniline, Nanoparticles, Nano-indentation, Corrosion resistance, Surface morphology

M. A. Alam (✉), U. A. Samad, E.-S. M. Sherif, A. Seikh, S. M. Al-Zahrani, N. H. Alharthi
Center of Excellence for Research in Engineering Materials (CEREM), King Saud University, P. O. Box 800, Riyadh 11421, Saudi Arabia
e-mail: moalam@ksu.edu.sa

E.-S. M. Sherif
Electrochemistry and Corrosion Laboratory, Department of Physical Chemistry, National Research Centre, El-Behoth St. 33, Dokki, Cairo 12622, Egypt

S. M. Al-Zahrani
Chemical Engineering Department, King Saud University, P.O. Box 800, Riyadh 11421, Saudi Arabia

M. Alam (✉)
Department of Chemistry, College of Science, King Saud University, P.O. Box 2455, Riyadh 11451, Saudi Arabia
e-mail: malamiitd@gmail.com

Introduction

Among electrically conducting polymers, polyaniline (PANI) has the potential to emerge as the most efficient corrosion-inhibiting pigment.[1] This polymer can be used to achieve high conductivity, and is stable for various applications.[2,3] Thin conducting films can be coated with the help of PANI, resulting in an improved adhesion on the substrate, and a stable system can be achieved using the base materials.[4,5] Therefore, PANI can substitute other corrosive and hazardous inhibiting pigments in various organic coatings, and impart better corrosion-inhibiting properties as compared to conventional paint formulations. Thus, this material can be incorporated and its performance in other organic or epoxy coatings examined to ensure the elimination of hazardous corrosion-inhibiting pigments presently used in coatings; in addition, its effect on the other properties of coating formulations can be elucidated.[4–6]

The effects of PANI on the coating formulation can be investigated through the incorporation with resin and other paint ingredients. The composition of the formulation after curing, which consists of a binder and other additives and pigments, produces a hard and durable film on the substrate. For this reason, PANI has been used along with all of the additives and ingredients of the formulation,[7–9] the compositions of

which affect the properties of this conducting polymer, and can be investigated through different techniques to establish the role of PANI in the final coating formulation. Chen and Liu[7] reported a novel approach to the development of PANI-containing coatings with waterborne corrosion protection through the preparation of spherical PANI/partially phosphorylated poly(vinyl alcohol) (PANI/P-PVA) nanoparticles using chemical oxidative dispersion polymerization in the presence of P-PVA. The authors[7] also reported the corrosion protection property of PANI/P-PVA-containing coatings on mild steel using salt spray test and the EIS method in a 3.0 wt% NaCl solution. Along with PANI, the inorganic pigments also had a vital effect. Therefore, it has become essential to study the impact of the inorganic pigments in the coating composition along with the polyaniline conducting polymer.[8–10] The incorporation of a PANI pigment with other inorganic corrosion-inhibiting pigments has been reported to provide corrosion-resistant properties in the coatings. The intention of such incorporation was to observe the effects of synergism of PANI and other species such as $Zn_3(PO_4)_2.2H_2O$ inorganic pigments.[10] Different coating formulations based on PANI and inorganic anticorrosive pigments have been developed to investigate the anticorrosion and adhesion properties of formulated coatings. The incorporation of PANI and Zn-powder, which is an electrochemically active pigment in the coating formulation, has been characterized and investigated to prove the synergism and anticorrosion efficiency of the coating system.[11]

The conductivity and thermal and electrochemical properties can be enhanced through the incorporation of different types of nanomaterials along with the PANI conducting polymer. Many materials can be used, including graphite, TiO_2, ZnO, ZrO_2, and SiO_2 nanoparticles.[12–15] In particular, ZnO, ZrO_2, and SiO_2 have been reported in a previously published article[16] as having increased the corrosion efficiency of the coating. The total effect or improvement may be associated with the strong bonding between inorganic and organic phases, as well as the interaction with the nanoparticles and PANI, which is expected to increase the mechanical and electrical properties of the nanocomposite produced.[15] The author attempted for the first time to produce PANI-based nanocomposites with the incorporation of inorganic nanoparticles of TiO_2, Ag, and Zn through the specific and well-known chemical vapor deposition method. The prepared coatings were investigated using corrosion resistance measurements, and the performances of various nanocomposites were compared. The results exhibited an enhancement in the corrosion protection efficiency of Ag-incorporated nano-coatings, which motivated our research towards the development of epoxy-matrix-based formulations.

We prepared different nanocomposites based on nano-pigments, Ag, TiO_2, and ZnO, with the incorporation of a polyaniline conducting polymer (PANI).[15] The corrosion behaviors of PANI, PANI/TiO_2, PANI/Ag, and PANI/Zn nanocomposite films were studied in a 3.5% NaCl solution. The comparison results were obtained by applying the Tafel extrapolation and EIS techniques. The findings indicate that PANI/Ag nanocomposite films yielded a higher protection efficiency (PE = 97.54%) compared to PANI (PE = 91.41%), PANI/TiO_2 (PE = 91.91%), and PANI/Zn (PE = 92.52%) nanocomposite films.[14] The results show that the addition of nanomaterials (TiO_2, Ag, and Zn) into the polymer matrix of PANI enhanced the electrical conductivity of the PANI/Zn film and the corrosion resistance of the polyaniline polymer. These findings were further confirmed through a decrease in the oxygen and water permeability, and an increase in the coating adhesion in the presence of TiO_2, Ag, and Zn nanomaterials, in the PANI. The EIS measurements indicate that the incorporation of TiO_2, Ag, and Zn into the coating increased both the charge transfer and the pore resistance. The highest protection efficiency was obtained for the PANI/Ag nanocomposite film (PE = 97.54%). This research motivated our work to produce the nanocomposites of PANI with Ag and ZnO, and to develop the formulations of their synergism to achieve balanced and improved corrosion resistance properties for offshore or splash zone applications.[14]

In this study, we intend to develop a coating containing conducting polymer (CP)-based nanocomposites (e.g., CP-inorganic parts and nano-pigments such as Ag and ZnO) as a substitution for hazardous inorganic materials such as zinc dust, zinc phosphate ($Zn_3(PO_4)_2$), and zinc chromates (Zn_3CrO_4) generally used in conventional epoxy coatings. The mechanical properties and corrosion resistance for the fabricated coatings have been investigated using different measurement methods. It was expected that the new synthesized coatings would have good mechanical properties and show excellent corrosion resistance in 3.5% NaCl solution.

Materials and methods

The fabricated epoxy coatings (S1–S4) were formulated as reported in our previous study.[1] The incorporation of Ag and ZnO nanoparticles (purchased from Sigma-Aldrich, USA) in epoxy coating formulations has also been applied using a mechanical mixer followed by a sonication technique. Silane was added to acetone and stirred for 5 min at a low rotation per minute (rpm). Nanoparticles Ag and ZnO were mixed into an acetone silane solution for at least 15 min to facilitate a complete dispersion of the nanoparticles. This prepared slurry of a silane/nanoparticle solution was mixed with an epoxy/conducting polymer mixture for at least 1.0 h at 4000 rpm using a mechanical stirrer. After the mixing was complete, sonication was performed for 60 min at 50°C. After sonication, the mixture was kept for stabilization for about 20 min.

After stabilization, a hardener was added to the epoxy/CP/nanoparticle mixture, and the mixing process was continued for at least 5–6 min at about 500 rpm using a mechanical stirrer. This modified slurry was coated onto various substrates for characterization using various techniques, taking into account that the mixture should be stabilized before being applied as a coating.

Attenuated total reflectance infrared spectroscopy (ATR-IR) measurements were used to study the crosslinking reactions of the epoxy resin, hardener, conducting polymer, and nanoparticles to fabricate the coatings samples (S1–S4). For this purpose, the epoxy coatings were formulated with a hardener and were applied for 1 week on small glass plates. The surface morphology of the coatings was investigated using a field-emission scanning electron microscope (FE-SEM, JEOL model JSM7600 F). The operating conditions for the employed FE-SEM were 5 kV with a working distance of 4.5 mm. The differential scanning calorimetry (DSC) technique was conducted using a TA Instrument SDT Q-600, which was calibrated according to the manufacturer's procedure (TA Instruments, Germany). The DSC tests were conducted at a heating rate of 10°C/min from room temperature to 120°C in a nitrogen atmosphere (50 ml/min). The effects of the nanoparticles on the mechanical properties, such as the hardness and modulus of elasticity, were evaluated using nano-indentation. The procedures for the nano-indentation tests were the same as those conducted in our previous work.[1] The anticorrosive performance of the epoxy coating system was investigated using electrochemical impedance spectroscopy (EIS) measurements in a conventional three-electrode cell, with Ag/AgCl (in a saturated KCl solution) as the reference electrode, stainless steel as the counter electrode, and steel-coated coupons as the working electrode. The area of the working electrode exposed to the test solution (3.5% NaCl solution) was 10 cm^2. The EIS data were collected using an Autolab Ecochemie PGSTAT 30 (Potentiostat/Galvanostat), and a frequency scan within the range of 100 kHz to 1.0 mHz was carried out by applying a ± 5 mV amplitude sinusoidal wave perturbation at the corrosion potential.

Results and discussion

ATR-IR measurement

ATR-IR investigations were carried out to report the dispersions of the epoxy resin, curing agent, PANI, and distribution of Ag and ZnO nanoparticles. The aim of using the ART-IR technique was also to characterize the chemical compositions of the synthesized epoxy coatings incorporating Ag and ZnO nanoparticles, where the epoxy coatings were applied on different glass plates and left for 7 days to be cured. The collected ATR-IR spectra for the different fabricated epoxy coatings incorporating nanoparticles of 0.2% Ag (S1), 0.4% Ag (S2), 0.2% Ag + 0.2% ZnO (S3), and 0.4% Ag + 0.4% ZnO (S4) are shown in Fig. 1. These spectra were obtained within a wide range of over 4000–500 cm^{-1} wave numbers to cover all spectra, which may appear for any functional groups of coatings. To focus on the area of most functional groups, ATR-IR spectra were also plotted within the range of 3500–2500 cm^{-1}, as depicted in Fig. 2.

It is well known that the combination between the D-3282 adduct as a hardener and DGEBA as an epoxy resin will yield various functional groups such as aromatic rings, including $-CH_3$, ≡ C–O–C ≡ , =C=O, –OH, $-NH_2$, and –N=N–. It can clearly be seen from Fig. 1 that numerous peaks appear on the spectra, namely 827, 1036, 1128, 1184, 1245, 1304, 1470, 1510, 1610, 1645, and 1708 cm^{-1} and as shown in Fig. 2, peaks at 2854, 2925, and 2962 cm^{-1}. Here, the spectra shown in the wave number range from 700 to 1800 cm^{-1}, which proves that there are aromatic rings, as indicated by the presence of the peaks within the region at 1400–1000 cm^{-1}, 1510 cm^{-1}, and 1609 cm^{-1}.[17–22] Evidence of the presence of C–H out-of-plane deformation vibration bands owing to the ring vibrations is indicated by the appearance of bands at 768 and 827 cm^{-1}.[17–22] This is in good agreement with a reported work[18–23] in which the chemical structure of DGEBA molecules has various organic groups, such as $-CH_3$, ≡ C–O–C ≡ , and aromatic rings, whereas mixing it with PANI would yield other groups, such as –N=N–, =C=O, –OH, and $-NH_2$. FTIR-ATR homogeneous peak distributions for the different fabricated coatings revealed the presence of all functional groups, which confirms the molecular structure for each synthesized coating.

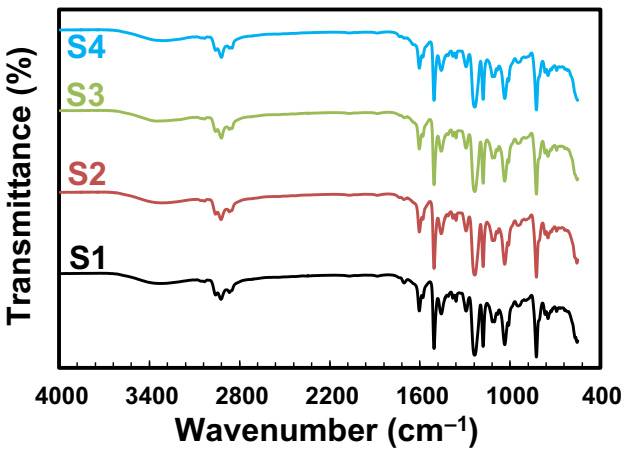

Fig. 1: ATR-IR spectra for the different fabricated epoxy coatings incorporating nanoparticles of 0.2% Ag (S1), 0.4% Ag (S2), 0.2% Ag + 0.2% ZnO (S3), and 0.4% Ag + 0.4% ZnO (S4)

FE-SEM investigations

The morphology and nano-distribution on the film surfaces were investigated using FE-SEM, the images of which are shown in Fig. 3. It can be seen that all fabricated coatings show a uniform, homogeneous, crack-free, and continuously close-packed structure and highly adherent film on the substrates, which is expected to lead to a good corrosion resistance of steel coated with these epoxy coatings incorporated with Ag and ZnO nanoparticles.

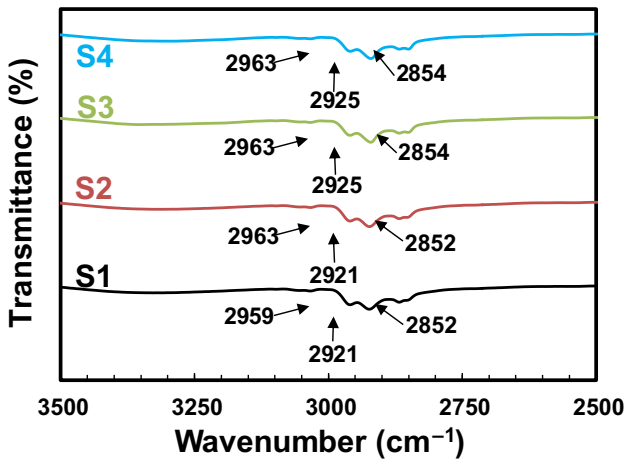

Fig. 2: ATR-IR spectra within the region of 3500–2500 cm^{-1} for the different fabricated epoxy coatings incorporated with the nanoparticles shown in Fig. 1

To confirm the composition of the fabricated coatings, the percentages of the elements found on the surface, and the distribution of these elements along with the added nanoparticles, i.e., Ag and ZnO, SEM images were collected for each element individually. Figure 4 shows the EDX profile and SEM images for the distribution of Ag and C on the surface, shown in Fig. 3a for the S1 epoxy coating. It can be seen from the EDX profile shown in Fig. 4 that the surface has C, Ag, and Cl, and there is no indication of the presence of other elements. This confirms that the coating layer is thick and completely covers the surface of the coated panel. In addition, the atomic percentages found on the surface of the S1 coating for C, O, and Ag were 80.49%, 19.36%, and 0.14%, respectively. The highest percentage is demonstrated for C, which is expected because the epoxy resin (DGEBA) and the curing agent (D-3282), as well as PANI, are hydrocarbon compounds that have carbon as the main component in their structure. The presence of O is attributed to the

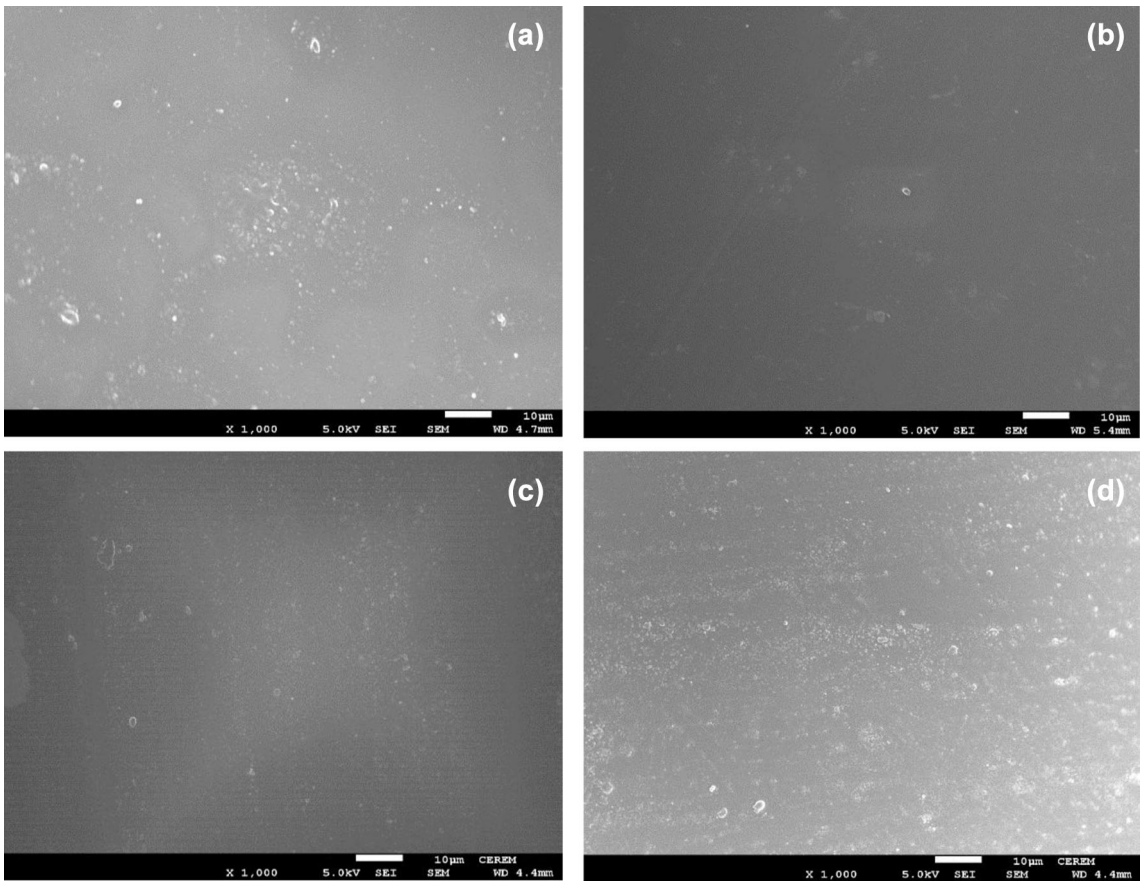

Fig. 3: FE-SEM images for (a) S1, (b) S2, (c) S3, and (d) S4 epoxy coatings incorporated with Ag and ZnO nanoparticles

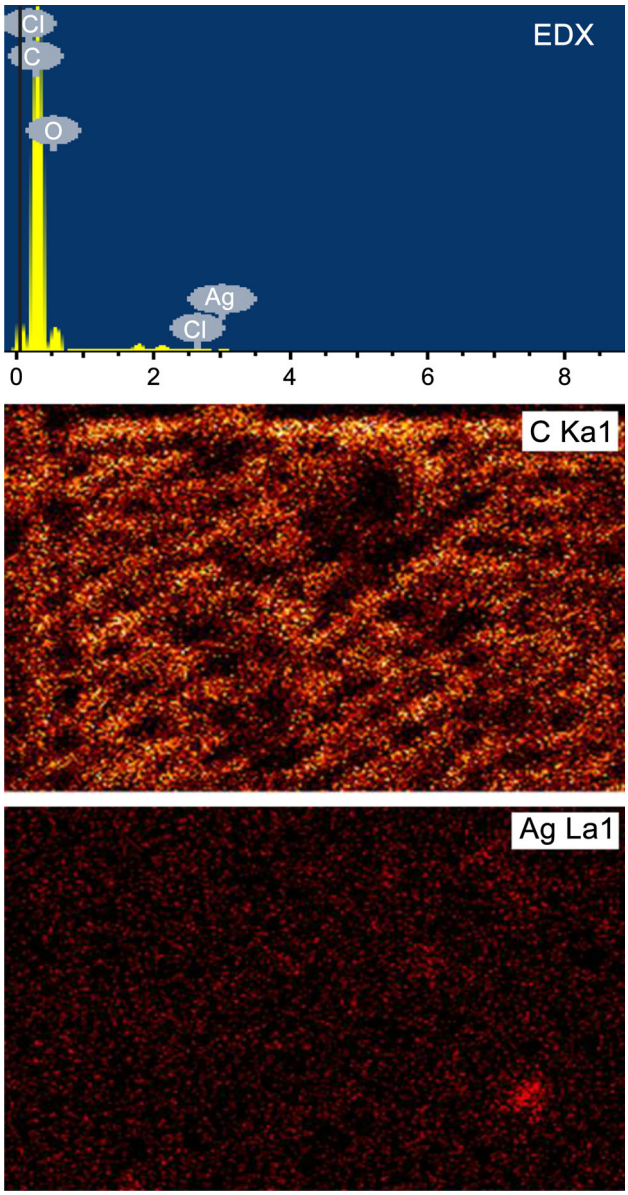

Fig. 4: EDX profile analysis and corresponding FE-SEM images for the distribution of C and Ag taken of the surface of S1 epoxy coating

formation of a passive layer that contains an oxide layer on the surface of the coating. In addition, the chloride ions (Cl^-) may have deposited on the surface of the coating, owing to the direct immersion of the coated panels in the NaCl test solution. The percentage of Ag (0.14%) is less than that originally present (0.2%), which is also due to the presence of a top passive layer on the surface of the coatings, thanks to its immersion in the test solution for 24 h. The FE-SEM mapping shown in Fig. 4 also confirms that C covers the majority of the surface, and with Ag, both are homogeneously distributed over the entire surface of the coating.

Figure 5 shows the EDX profile analysis and corresponding FE-SEM images for the distribution of O, Ag, and Zn taken of the surface of S4 epoxy coating. This was to report the percentage and distribution of O, Ag, and Zn. The EDX profile (Fig. 6) reveals the presence of C, O, Ag, and Zn; the percentages of these components are 80.0%, 19.6%, 0.2%, and 0.4%, respectively. Still, C represents the majority of the elements found on the surface of the coating, whereas the percentage of O is approximately 20%, which is confirmed by its dense distribution, as depicted by the FE-SEM mapping for O, as shown in Fig. 5. The percentages of Ag and Zn are the lowest because they were originally low (0.4%), and because of the coverage of the surface of the coating using a passive layer. The homogeneous distribution of both Ag and Zn, as shown in Fig. 6, confirms the good fabrication of the reported nanoparticles incorporated in epoxy coatings. The results of SEM/EDX investigations are thus in good agreement with the results obtained from ATR-IR spectra.

Nano-indentation analysis

The modulus and hardness properties upon incorporation of the nanoparticles were studied using the nano-test platform from Micro Materials, UK, with a complete software package and a Berkovich diamond indenter. The maximum load applied for all samples was 250 mN, and the results of 20 indentations conducted at different locations to obtain acceptable values of hardness (H) and elastic modulus (E) were averaged. The hardness and elastic modulus were calculated according to Oliver and Pharr's[24] method through equations (1) and (2):

$$H = \frac{F_{\max}}{A_c} \tag{1}$$

where H = hardness, $F_{\max}$ = maximum applied, and A_c = projected contact area.

$$\frac{1}{E_r} = \frac{1-v^2}{E} + \frac{1-v_i^2}{E_i} \tag{2}$$

Here, A_c is the projected contact area, and E_r is the reduced modulus. In addition, E and E_i are the elastic modulus of the sample, and indenters v and v_i are the Poisson's ratio of the sample and diamond indenter, respectively.

The load–displacement curve for epoxy coatings contains different amounts of nanoparticles and is shown in Fig. 6. As clearly shown, at the maximum load of 250 mN, the penetration depths are reduced. The maximum penetration depth of 9671 nm was recorded for the S1 sample, whereas the minimum penetration depth was observed for S2 (8853 nm). The

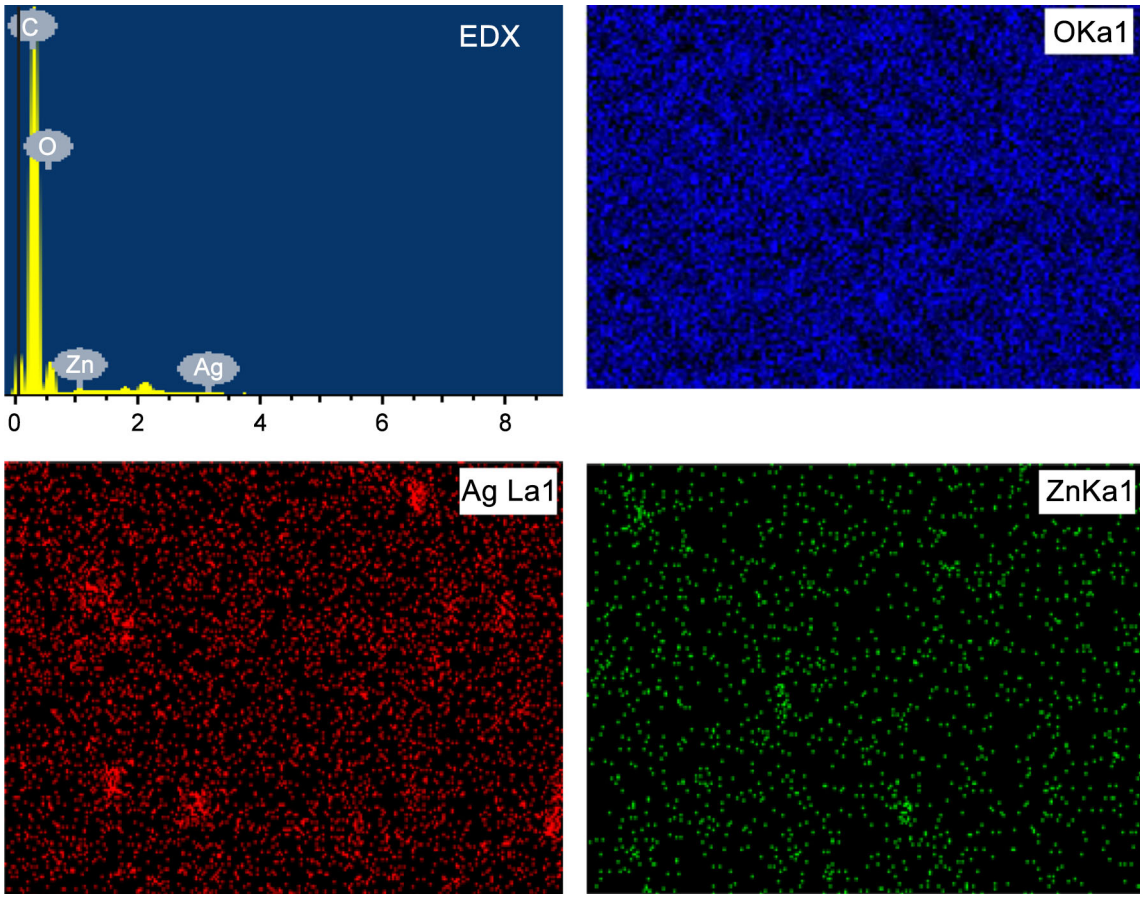

Fig. 5: EDX profile analysis and corresponding FE-SEM images for the distribution of O, Ag, and Zn taken of the surface of S4 epoxy coating

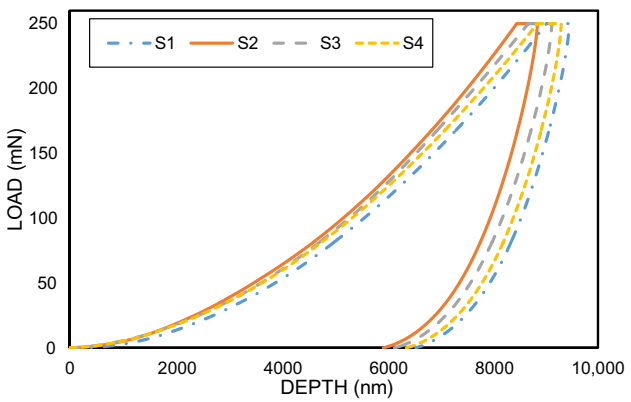

Fig. 6: Load vs. displacement curves with different percentages of nanoparticle loading

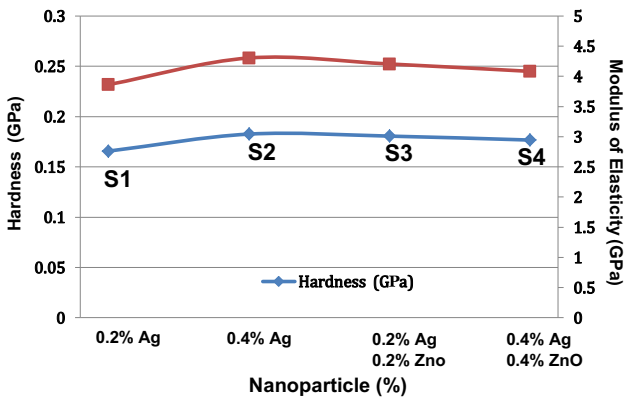

Fig. 7: Nano-indentation analysis for the fabricated coatings, which were incorporated using 0.2% Ag (S1), 0.4% Ag (S2), 0.2% Ag + 0.2% ZnO (S3), and 0.4% Ag + 0.4% ZnO (S4) nanoparticles

movement of the penetration depth to lower values implies an improvement in the hardness values because of an improvement in the load-bearing capacity of the prepared coatings.[25]

Figure 7 shows the elastic modulus and hardness of the studied coatings, where the improvement in the nano-mechanical properties can be seen in Table 1, in which the hardness values with the addition of an equal proportion of nanoparticles (ZnO and Ag) are increased. The results show an increase in elastic modulus and hardness of the coatings from S1 to S4 because of the dual nanoparticle effect. The addition of 0.4% Ag nanoparticles provides the maximum hard-

Table 1: Hardness and reduced modulus recorded for the fabricated epoxy coatings containing Ag and ZnO nanoparticles

Sample	Nanoparticles		Hardness (GPa)	Reduced modulus (GPa)
	Ag (%)	ZnO (%)		
S1	0.2	0.0	0.16	3.86
S2	0.4	0.0	0.18	4.30
S3	0.2	0.2	0.18	4.20
S4	0.4	0.4	0.18	4.08

Table 2: Dry film thickness, pendulum hardness, scratch resistance, and impact strength values of Ag and ZnO incorporated epoxy coatings

Sample	PANI%	Nanoparticle		Dry film thickness (μm)	Pendulum hardness	Scratch resistance (Kg)	Impact strength (in/lb)
		Ag%	ZnO%				
S1	0.78	0.2	0.0	60–80	108	5.5	64
S2	0.78	0.4	0.0	60–80	117	6.0	72
S3	0.78	0.2	0.2	60–80	111	7.0	96
S4	0.78	0.4	0.4	60–80	100	7.5	96

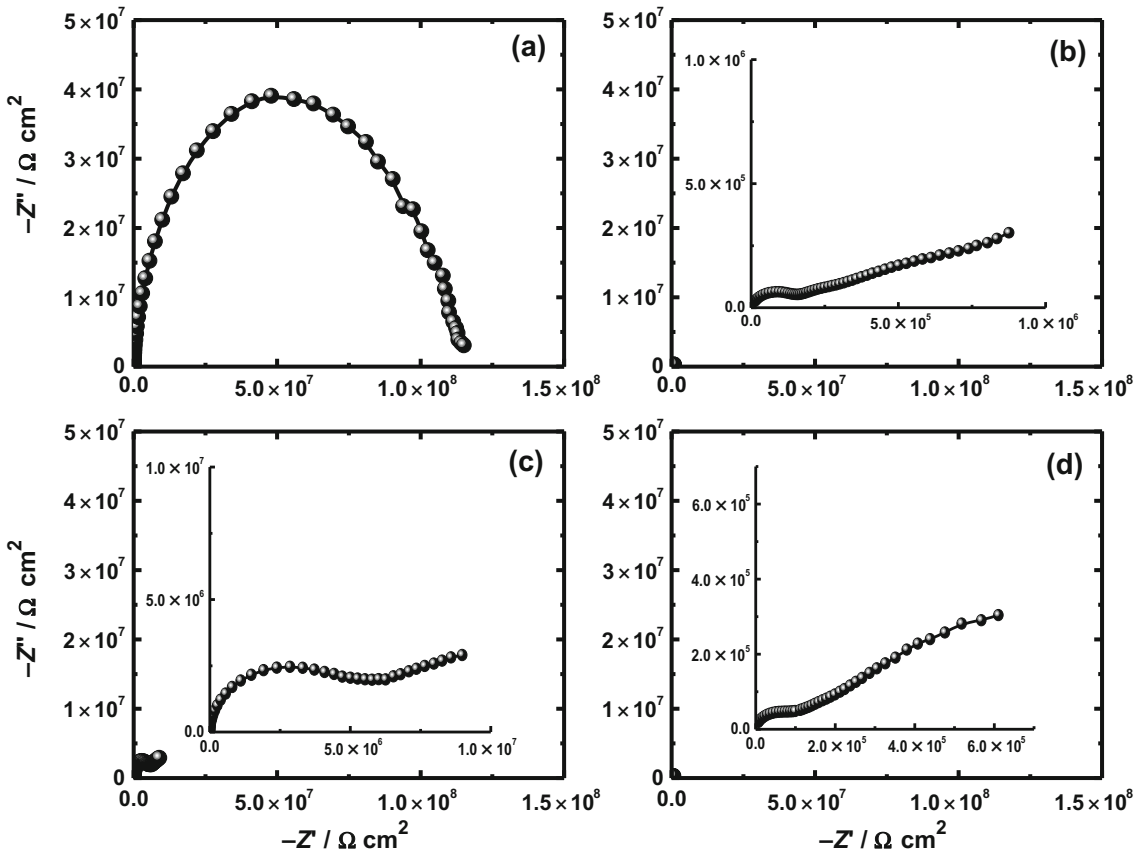

Fig. 8: Nyquist plots obtained for (a) S1, (b) S2, (c) S3, and (d) S4 epoxy coating incorporated Ag and ZnO nanoparticles after 24-h immersion in 3.5% NaCl solution

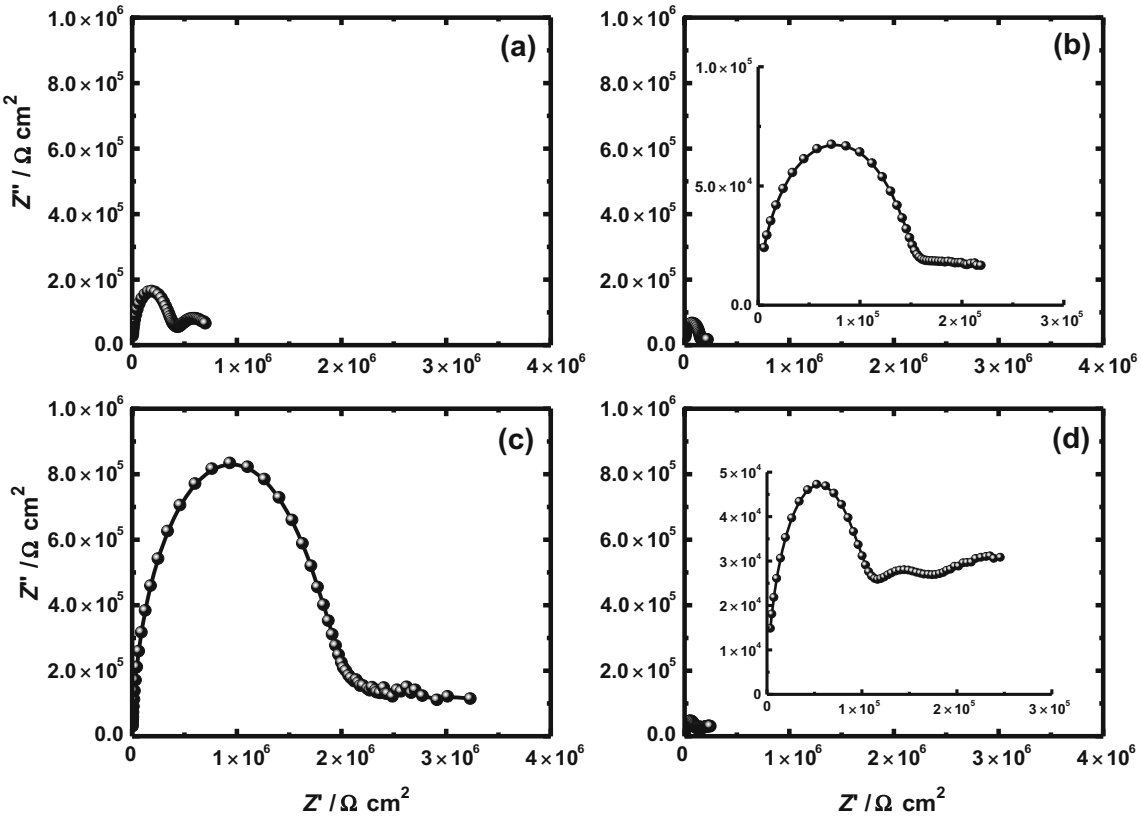

Fig. 9: Nyquist plots obtained for (a) S1, (b) S2, (c) S3, and (d) S4 epoxy coating incorporated Ag and ZnO nanoparticles after 168-h immersion in 3.5% NaCl solution

ness of 0.18 GPa and modulus of 4.30 GPa for the S2 sample, whereas the synergism of the nanoparticles at a 0.2% ratio (sample S3) provides the best values of 0.18 GPa for the hardness and 4.20 GPa for the modulus. The obtained values of nano-indentation are in accordance with conventional test results mentioned in Table 2, where the maximum mechanical properties were obtained for the S2 sample.

Electrochemical impedance spectroscopy (EIS)

EIS measurements have been successfully employed to report the kinetic parameters for the electron transfer at the surface/electrolyte interface.[26–33] The Nyquist plots obtained for (a) S1, (b) S2, (c) S3, and (d) S4 epoxy coating incorporated Ag and ZnO nanoparticles after 24-h immersion in a 3.5% NaCl solution are shown in Fig. 8. It can be seen that the epoxy coating containing 0.2% Ag (S1) showed only one semicircle with a very wide diameter. Increasing the percentage of Ag in the coating from 0.2% (S1) to 0.4% (S2) changed the shape of the spectrum to a small semicircle and a long segment. The highest values for Z' and Z'' are shown for the S3 sample, which has 0.2% Ag and 0.2% ZnO, indicating that the presence of Ag and ZnO at these percentages increases the corrosion resistance of the epoxy coating.

To shed additional light on the corrosion behavior of the fabricated coatings after long immersion periods, EIS measurements were carried out after 168 and 720 h, the spectra of which are shown in Figs. 9 and 10, respectively. Figures 8 and 9 indicate that an elongation of the immersion time from 24 to 168 h decreases the corrosion resistance through a decrease in the values of the spectra obtained, which is most probably due to the slight degradation of the coatings with time. Further increasing the immersion time to 720 h before the measurements decreased the values of both the real and imaginary resistances through a decrease in the diameter of the semicircles. It is believed that the corrosion resistance of the coatings increases in the presence of both Ag and ZnO nanoparticles, which is obvious for the epoxy coating containing 0.2% Ag and 0.2% ZnO nanoparticles, namely S3, and 0.4% Ag and 0.4% ZnO nanoparticles, namely S4. This result comes from a synergetic effect occurring between the epoxy coating and Ag along with the ZnO nanoparticles, and thus the presence of Ag and ZnO nanoparticles strengthen the mechanical properties of the coatings and increase the resistance against corrosion in 3.5% NaCl solution.

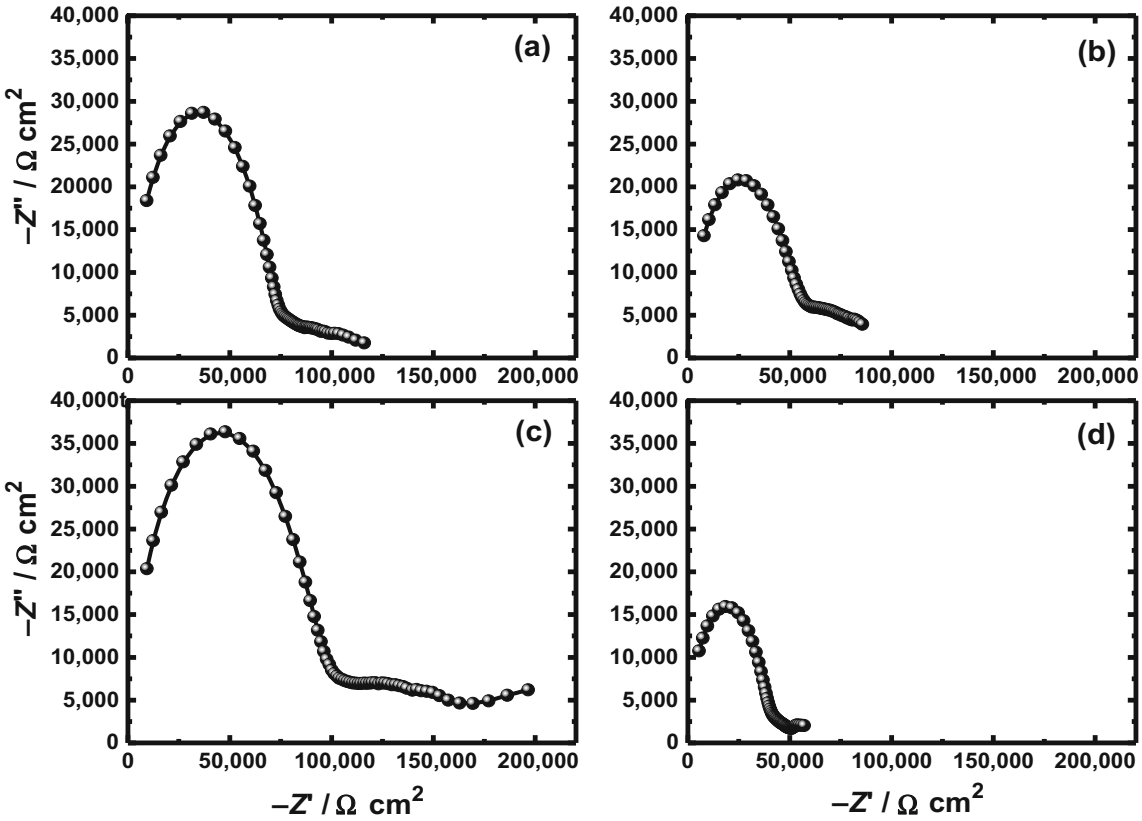

Fig. 10: Nyquist plots obtained for (a) S1, (b) S2, (c) S3, and (d) S4 epoxy coating incorporated Ag and ZnO nanoparticles after 24-h exposure in 3.5% NaCl solution

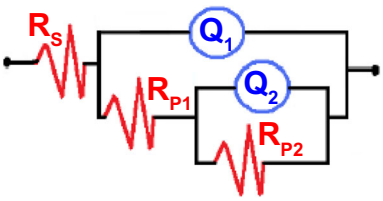

Fig. 11: Equivalent circuit model employed to fit the impedance data shown in Figs. 8, 9, and 10

To quantify the effect of Ag and ZnO nanoparticles on the corrosion resistance of epoxy coatings, the data obtained from EIS plots for the coatings after immersion for different exposure periods were best fitted to an equivalent circuit, which is shown in Fig. 11. The values of the impedance parameters obtained from the fitting of the EIS data to the equivalent circuit shown in Fig. 11 are listed in Table 3. The circuit consists of a solution resistance (R_S), constant phase elements (Q_1), polarization resistance (R_{P1}), another constant phase element (Q_2), and a second polarization resistance (R_{P2}). It is clear from Table 3 that Q_1 represents a typical double-layer capacitor with significant porosities because their n_1 values are close to 1. Here, R_{P1} can be considered as the charge transfer resistance representing the polarization resistance between the epoxy coatings and the solution interface, and R_{P2} is the polarization resistance between a corrosion product layer and/or an oxide film and the solution, and the overall polarization resistance is obtained from the parallel combination of R_{P1} and R_{P2}.[30,31] The Q_2 values have characteristics of a Warburg with their n_2 values at approximately 0.5, which indicates that the surface of the fabricated coatings have high corrosion resistance. The EIS data thus confirm that the accelerated corrosion assays using an aggressive 3.5% saline solution revealed that the panels coated with PANI-based epoxy coatings (a synergism of Ag and ZnO nanoparticles, S1–S4) are significantly more resistant against corrosion than those protected with conventional epoxy coatings. Moreover, epoxy nanocomposite coatings combine the advantages of a synergism of epoxy, polyaniline, and Ag + ZnO nanoparticles (S1–S4). Among them, the corrosion resistance of epoxy coating S3 recorded the highest resistance compared with the other coatings, and was far better compared to the conventional epoxy coatings incorporated with polyaniline even over long periods of immersion time, namely 168 and 720 h, in a corrosive NaCl medium.

Table 3: EIS parameters obtained by fitting the Nyquist plots for the epoxy coatings immersed in 3.5% NaCl solutions for 24 h, 168 h, and 720 h, respectively

Sample	Parameters						
	R_S/Ω	Q_1		R_{P1}/k Ω	Q_2		R_{P2}/k Ω
		$Y_{Q1}/\mu F$	n_1		$Y_{Q2}/\mu F$	n_2	
S1-24h	476	780	0.96	23,700	252	0.51	94,300
S2-24h	473	881	0.95	80.3	140	0.28	3180
S3-24h	904	547	0.97	4160	92.3	0.39	32,300
S4-24h	675	213	0.91	73.3	104	0.38	5910
S1-168h	622	101	0.94	340	152	0.37	544
S2-168h	363	115	0.94	146	188	0.50	93.0
S3-168h	936	392	0.91	100	748	0.95	45,100
S4-168h	599	122	0.98	68.7	254	0.28	268
S1-720h	865	285	0.86	66.2	181	0.24	60.6
S2-720h	562	339	0.87	44.6	90.2	0.27	52.2
S3-720h	1090	322	0.85	88.4	105	0.28	117
S4-720h	232	308	0.91	15.2	122	0.09	63.4

Conclusions

Four epoxy/2pack coatings containing PANI and incorporated Ag and ZnO nanoparticles were manufactured. ATR-FTIR and SEM/EDX techniques were employed to confirm the chemical composition and surface morphology for the coatings obtained. The pendulum hardness, scratch resistance, and impact strength were measured to report the mechanical properties along with a nano-indentation to report the indentation hardness and modulus of the fabricated coatings. The corrosion behavior using EIS measurements for the fabricated coatings in 3.5% NaCl solutions after various immersion periods of time was also studied. It was found that the presence of Ag and ZnO nanoparticles improves the mechanical properties and increases the corrosion resistance for the manufactured coatings. The corrosion resistance recorded high values even after prolonging the immersion time in the NaCl solution for 168 and 720 h. The increase in corrosion resistance was due to a combination of the synergistic effect between nanoparticles (Ag and ZnO) and PANI, along with the epoxy resin components (DGEBA and D-3282).

Acknowledgment The authors would like to extend their sincere appreciation to the Deanship of Scientific Research at King Saud University for its funding of this research through the Research Group Project No. RGP-160.

References

1. Samad, UA, Alam, MA, Sherif, El-Sayed M, Alothman, O, Seikh, AH, Al-Zahrani, SM, ''Manufacturing and Characterization of Corrosion Resistant Epoxy/2Pack Coatings Incorporated with Polyaniline Conductive Polymer.'' *Int. J. Electrochem. Sci.*, **10** 5599–5613 (2015)
2. Samui, AB, Phadnis, SM, ''Manufacturing and Characterization of Corrosion Resistant Epoxy/2Pack Coatings Incorporated with Polyaniline Conductive Polymer.'' *Prog. Org. Coat.*, **54** 263–267 (2005)
3. Sathiyanarayanan, S, Muthukrishnan, S, Venkatachari, G, Trivedi, DC, ''Corrosion Protection of Steel by Polyaniline (PANI) Pigmented Paint Coating.'' *Prog. Org. Coat.*, **53** (4) 297–301 (2005)
4. Abu, YM, Aoki, K, ''Corrosion Protection by Polyaniline-Coated Latex Microspheres.'' *J. Electroanal. Chem.*, **583** (1) 133–139 (2005)
5. Luo, K, Shi, N, Sun, C, ''Thermal Transition of Electrochemically Synthesized Polyaniline.'' *Polym. Degrad. Stab.*, **91** (11) 2660–2664 (2006)
6. Mathiazhagan, A, Joseph, R, ''Nanotechnology—A New Prospective in Organic Coating—Review.'' *Int. J. Chem. Eng. Appl.*, **2** (4) 225–237 (2011)
7. Chen, F, Liu, P, ''Conducting Polyaniline Nanoparticles and Their Dispersion for Waterborne Corrosion Protection Coatings.'' *ACS Appl. Mater. Interfaces*, **3** (7) 2694–2702 (2011)
8. Abdiryim, T, Gang, ZX, Jamal, R, ''Comparative Studies of Solid-State Synthesized Polyaniline Doped with Inorganic Acids.'' *Mater. Chem. Phys.*, **90** (2–3) 367–372 (2005)
9. Kalendov, A, Kalenda, P, Vesely, D, ''Comparison of the Efficiency of Inorganic Nonmetal Pigments with Zinc Powder in Anticorrosion Paints.'' *Prog. Org. Coat.*, **57** (1) 1–10 (2006)
10. Amo, BD, Romagnoli, R, Vetere, VF, Herńandez, LS, ''Study of the Anticorrosive Properties of Zinc Phosphate in Vinyl Paints.'' *Prog. Org. Coat.*, **33** (1) 28–35 (1998)
11. Kalendová, A, ''Effects of Particle Sizes and Shapes of Zinc Metal on the Properties of Anticorrosive Coatings.'' *Prog. Org. Coat.*, **46** (4) 324–332 (2003)
12. Hermas, AEA, Salam, MA, Al-Juaid, SS, ''In Situ Electrochemical Preparation of Multi-walled Carbon Nanotubes/Polyaniline Composite on the Stainless Steel.'' *Prog. Org. Coat.*, **76** (12) 1810–1813 (2013)

13. Hu, ZA, Xie, YL, Wang, YX, Mo, LP, Yang, YY, Zhang, ZY, ''Polyaniline/SnO_2 Nanocomposite for Supercapacitor Applications.'' *Mater. Chem. Phys.*, **114** (2–3) 990–995 (2009)
14. Gomez, H, Ram, MK, Alvi, F, Stefanakos, E, Kumar, A, ''Novel Synthesis, Characterization, and Corrosion Inhibition Properties of Nanodiamond–Polyaniline Films.'' *J. Phys. Chem. C.*, **114** (44) 18797–18804 (2010)
15. Ates, M, Topkayaa, E, ''Nanocomposite Film Formations of Polyaniline via TiO2, Ag, and Zn, and Their Corrosion Protection Properties.'' *Prog. Org. Coat.*, **82** 33–40 (2015)
16. Alam, MA, Samad, UA, Khan, R, Alam, M, Al-Zahrani, SM, ''Anti-corrosive Performance of Epoxy Coatings Containing Various Nano-Particles for Splash Zone Applications.'' *Korean J. Chem. Eng.*, **34** (8) 2301–2310 (2017)
17. Shen, L, Wang, L, Liu, T, Chaobin, H, ''Nanoindentation and Morphological Studies of Epoxy Nanocomposites.'' *Macromol. Mater. Eng.*, **291** (11) 1358–1366 (2006)
18. Alam, MA, Sherif, El-Sayed M, Al-Zahrani, SM, ''Nanoindentation and Morphological Studies of Epoxy Nanocomposites.'' *Int. J. Electrochem. Sci.*, **8** 8388–8400 (2013)
19. Wang, Y, Jing, X, ''Preparation of an Epoxy/Polyaniline Composite Coating and Its Passivation Effect on Cold Rolled Steel.'' *Polym. J.*, **36** 374–379 (2004)
20. Armelin, E, Meneguzzi, Á, Carlos, AF, Carlos, A, ''Preparation of an Epoxy/Polyaniline Composite Coating and Its Passivation Effect on Cold Rolled Steel.'' *Surf. Coat. Tech.*, **203** (24) 3763–3769 (2009)
21. Alam, MA, Samad, UA, Sherif, El-Sayed M, Alothman, O, Seikh, AH, Al-Zahrani, SM, ''Effects of Minor Additions of Polypyrrole on the Thermal, Mechanical and Electrochemical Properties of Epoxy-2Pack Coatings.'' *Int. J. Electrochem. Sci.*, **12** 74–89 (2017)
22. Saravanan, K, Sathiyanarayanan, S, Muralidharan, S, Azim, SS, Venkatachari, G, ''Performance Evaluation of Polyaniline Pigmented Epoxy Coating for Corrosion Protection of Steel in Concrete Environment.'' *Prog. Org. Coat.*, **59** (2) 160–167 (2007)
23. Wetzel, B, Haupert, F, Zhang, MQ, ''Epoxy Nanocomposites with High Mechanical and Tribological Performance.'' *Composite Sci. Technol.*, **63** (14) 2055–2067 (2003)
24. Oliver, W, Pharr, G, ''An Improved Technique for Determining Hardness and Elastic Modulus Using Load and Displacement Sensing Indentation Experiments.'' *J. Mater. Res.*, **7** (6) 1564–1583 (1992)
25. Khan, R, Azhar, MA, Anis, A, Alam, MA, Boumaza, M, Al-Zahrani, SM, ''Facile Synthesis of Epoxy Nanocomposite Coatings Using Inorganic Nanoparticles for Enhanced Thermo-Mechanical Properties: A Comparative Study.'' *J. Coat. Technol. Res.*, **13** (1) 159–169 (2016)
26. Alharthi, N, Sherif, El-Sayed M, Abdo, HS, El-Abedin, SZ, ''Effect of Nickel Content on the Corrosion Resistance of Iron-Nickel Alloys in Concentrated Hydrochloric Acid Pickling Solutions.'' *Adv. Mater. Sci. Eng.* (2017). Article ID 1893672, 8 pages. https://doi.org/10.1155/2017/1893672
27. Sherif, El-Sayed M, El-Danaf, EA, Abdo, HS, El-Abedin, SZ, Al-Khazraji, H, ''Effect of Annealing Temperature on the Corrosion Protection of Hot Swaged Ti-54M Alloy in 2M HCl Pickling Solutions.'' *Metals*, **7** (1) 29–41 (2017)
28. Sherif, El-Sayed M, Abdo, HS, El Abedin, SZ, ''Electrochemical Corrosion Behavior of Fe64/Ni36 and Fe55/Ni45 Alloys in 4.0% Sodium Chloride Solutions.'' *Int. J. Electrochem. Sci.*, **12** 1600–1611 (2017)
29. Seikh, AH, Halfa, H, Sherif, El-Sayed M, ''Corrosion Resistance Performance of Newly Developed Cobalt-Free Maraging Steel Over Conventional Maraging Steel in Acidic Media.'' *Adv. Mater. Proc. Technol.*, **2** 283–292 (2016)
30. AlOtaibi, A, Sherif, El-Sayed M, Zinelis, S, Al-Jabbari, Y, ''Corrosion Behavior of Two cp Titanium Dental Implants Connected by Cobalt Chromium Metal Superstructure in Artificial Saliva and the Influence of Immersion Time.'' *Inter. J. Electrochem. Sci.*, **11** 5877–5890 (2016)
31. Gopi, D, Sherif, El-Sayed M, Surendiran, M, Sakila, DMA, Kavitha, L, ''Corrosion Inhibition by Benzotriazole Derivatives and Sodium Dodecyl Sulphate as Corrosion Inhibitors for Copper in Ground Water at Different Temperatures.'' *Surf. Interf. Anal.*, **47** (5) 618–625 (2015)
32. Sherif, EM, Park, SM, ''Effects of 1,4-naphthoquinone on Aluminum Corrosion in 0.50 M sodium chloride solutions.'' *Electrochim. Acta.*, **51** (7) 1313–1321 (2006)
33. Rehim, SSA, Hassan, HH, Amin, MA, ''Corrosion and Corrosion Inhibition of Al and Some Alloys in Sulphate Solutions Containing Halide Ions Investigated by an Impedance Technique.'' *Appl. Surf. Sci.*, **187** (3–4) 279–290 (2002)